Supporting information (SI)

Controlled Synthesis of Hierarchical Hollow $Co_xNi_{3-x}S_4$ towards Enhanced Rate Capability and Excellent Cycling Stability

Xiankun Xiong [a, b], Chaochao Lu [b], Zhongliang Pi [b], CunYuan Pei [a*], Cheng Du [b*]

[a]*College of Materials & Chemical Engineering, China Three Gorges University, Yichang, 443002, China*

[b]*Hubei Key Lab for Processing and Application of Catalytic Materials, College of Chemistry and Chemical Engineering, Huanggang Normal University, Huanggang, 437000, China*

*Corresponding author.
E-mail: 1154917949@qq.com; ducheng20141020@163.com

Physical characterizations

TEM images were obtained using a FEI Tecnai G2 F20 transmission microscope. SEM images were obtained by a Zeiss Sigma scanning electron microscope. Powder X-ray diffraction (XRD) patterns were measured by a Lab-XRD 6100 using Cu K_α radiation with a scan rate of $2°\cdot min^{-1}$. X-ray photoelectron spectroscopy (XPS) measurement was carried out with Thermo ESCALAB 250XI spectrometer equipped with Al K_α radiation (1486.6 eV).

Electrochemical measurement

To assess the electrochemical performance of the $Co_xNi_{3-x}S_4$ electrode materials, cyclic voltammetry (CV), galvanostatic charge-discharge (GCD), and electrochemical impedance spectroscopy (EIS) were conducted on a CHI 660E workstation (Shanghai Chenhua). The tests utilized a 6 M KOH solution as the electrolyte, with platinum foil as the counter electrode and a Hg/HgO electrode as the reference.

For the working electrode preparation, $Co_xNi_{3-x}S_4$ active material, conductive

carbon black, and polytetrafluoroethylene (PTFE) binder were mixed in a mass ratio of 75:20:5 and thoroughly ground. The resulting paste was evenly coated onto a nickel foam substrate (1 cm × 2 cm) to achieve a mass loading of approximately 2 mg·cm $^{-2}$.

The specific capacitance (C_F, F g^{-1}) and gravimetric specific capacity value (C_m, mAh g^{-1}) were calculated from the GCD curves using the following equations:

$$C_m = I \times \Delta t / (3.6m) \quad \text{(S1)}$$

$$C_F = I \times \Delta t / (m \times \Delta V) \quad \text{(S2)}$$

where I (A), Δt (s), m (g) and ΔV (V) donates to discharge current, discharge time, the mass of active material and the discharge voltage, respectively.

For asymmetric supercapacitors, the activated carbon derived from lotus pollen (AC) was used as negative electrode. The mass ratio of $Co_xNi_{3-x}S_4$ and AC was calculated using following equation:

$$\frac{m_+}{m_-} = \frac{C_- \times V_-}{3.6 \times C_+} \quad \text{(S3)}$$

where m (g) corresponds to actual mass of active material on the electrode, V_- is the potential window of AC electrode. C_+ (mAh·g^{-1}) is the gravimetric specific capacity of Co_xNi_yS electrode. C_- (F·g^{-1}) is the specific capacitance of AC electrode.

The corresponding energy density (E, Wh·kg^{-1}) and power density (P, W·kg^{-1}) were calculated using the following Equation (S4) and (S5).

$$E = \frac{C \times \Delta V^2}{2 \times 3.6} \quad \text{(S4)}$$

$$P = \frac{E \times 3600}{\Delta t} \quad \text{(S5)}$$

Where ΔV, C and Δt are the potential window, specific capacitance and discharge time, respectively.

These electrochemical measurements have been repeated at least three times to ensure the accuracy of data.

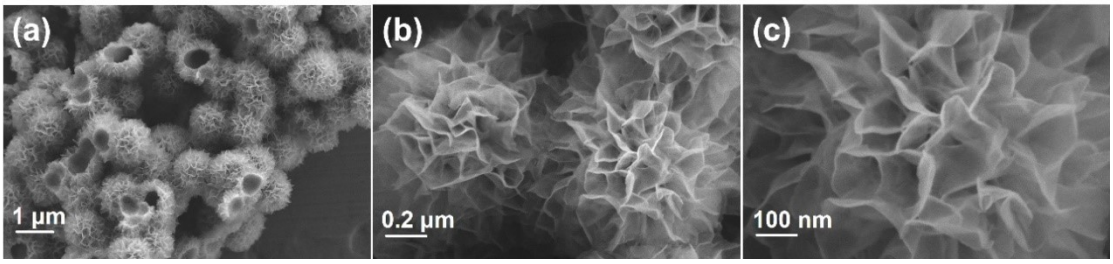

Fig. S1. SEM images of Co_1Ni_2-precusor

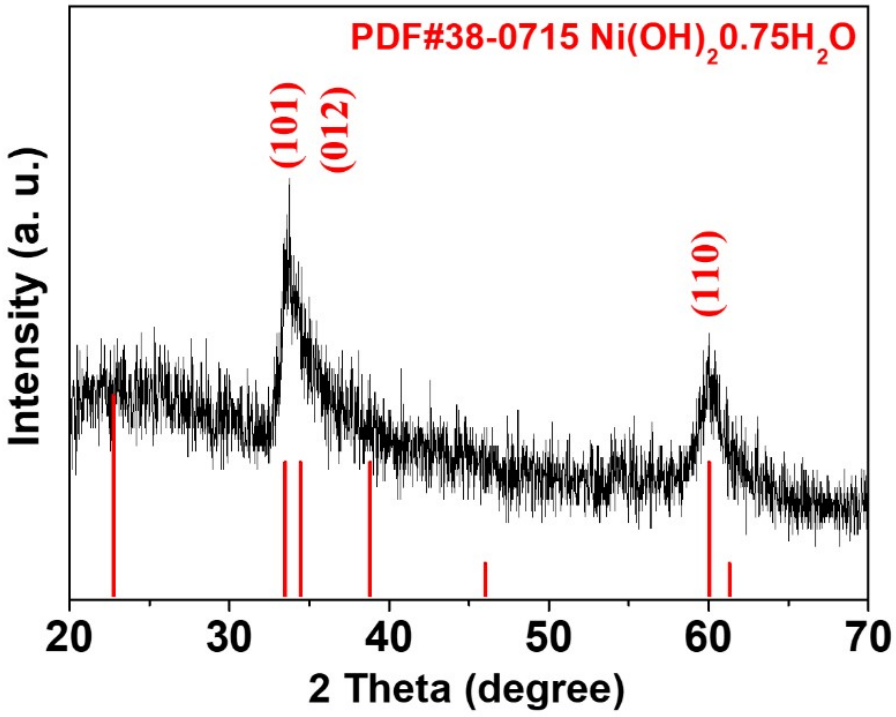

Fig. S2. XRD for Co_1Ni_2-precusor

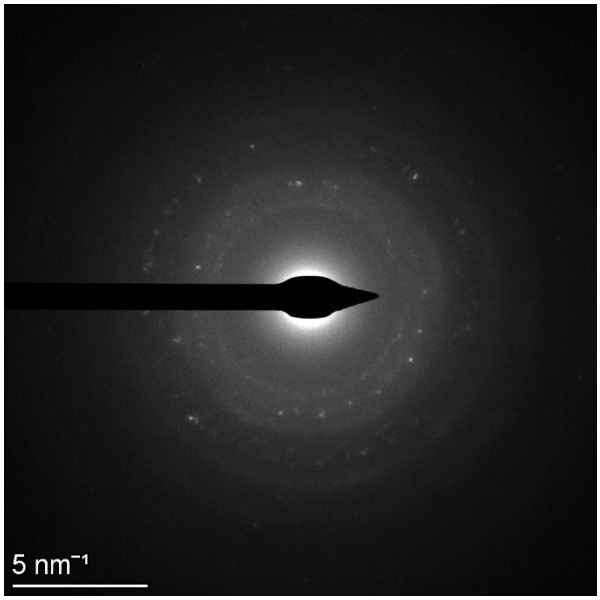

Fig. S3. SAED patterns of the $(Co_1Ni_2)S_4$

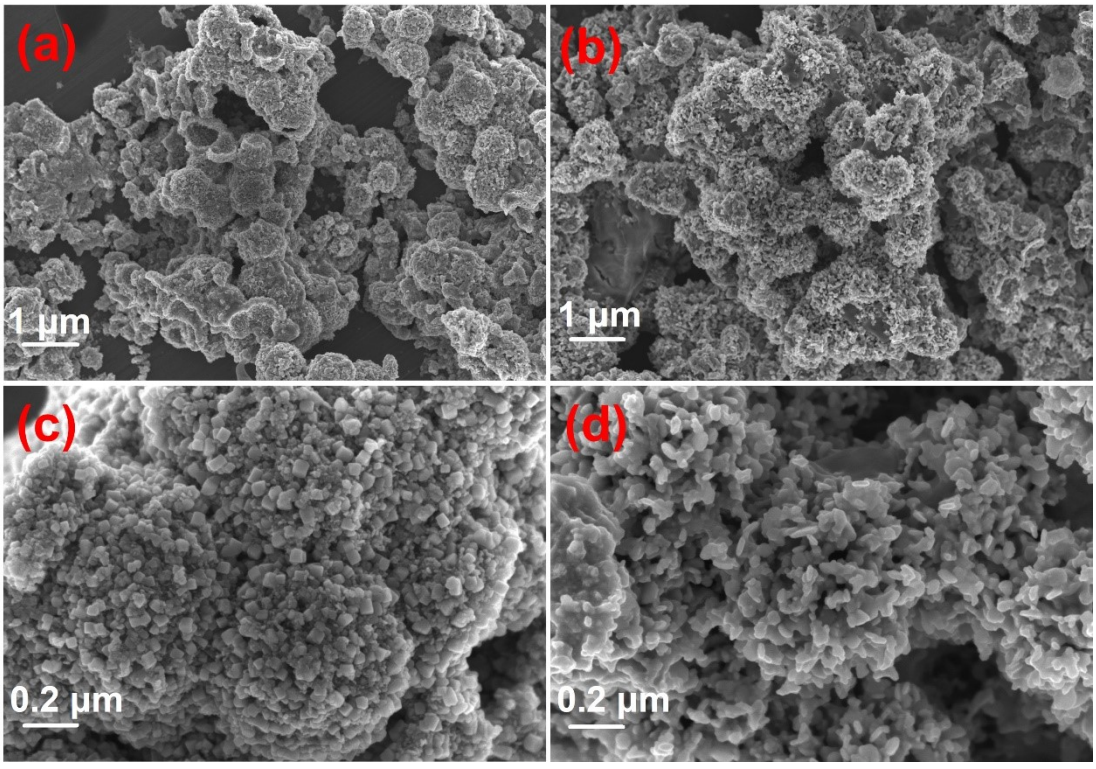

Fig. S4. SEM images of CoS (a, c) and NiS (b, d)

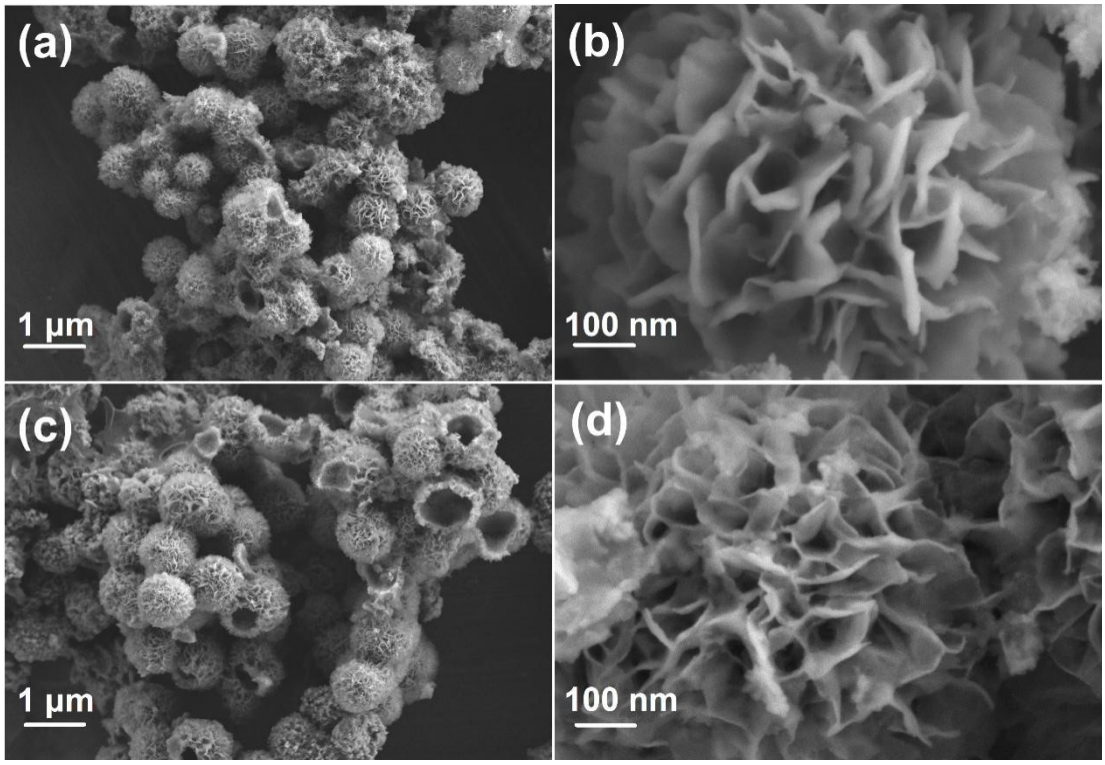

Fig. S5. SEM images of $(Co_{1.5}Ni_{1.5})S_4$ (a, b) and $(Co_{0.6}Ni_{2.4})S_4$ (c, d)

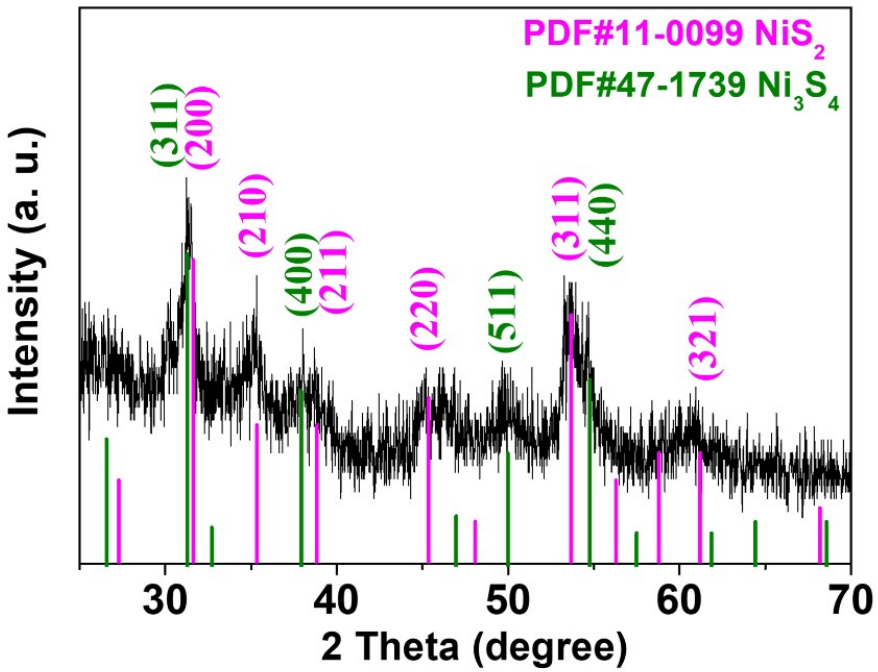

Fig. S6. XRD for NiS

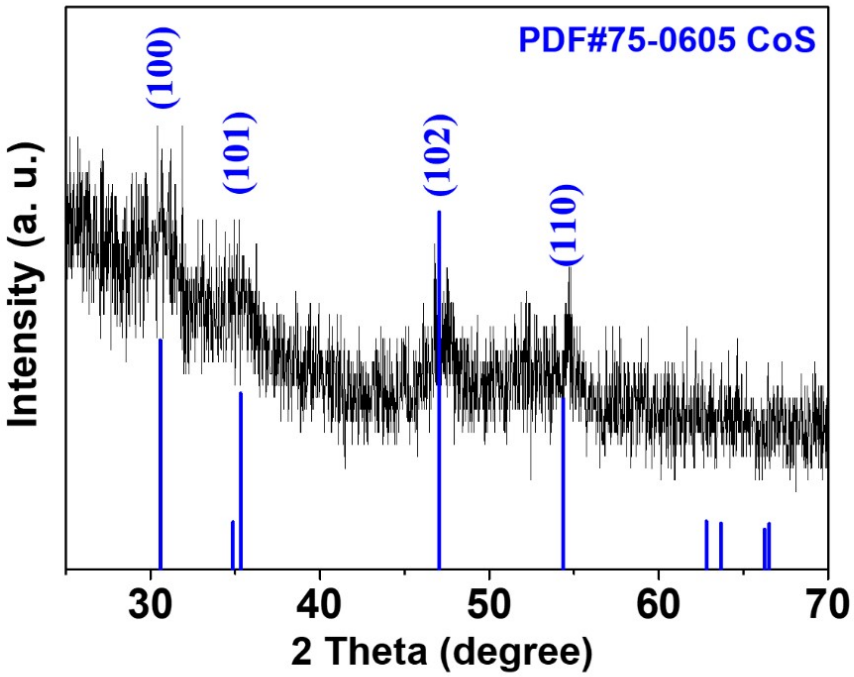

Fig. S7. XRD for CoS

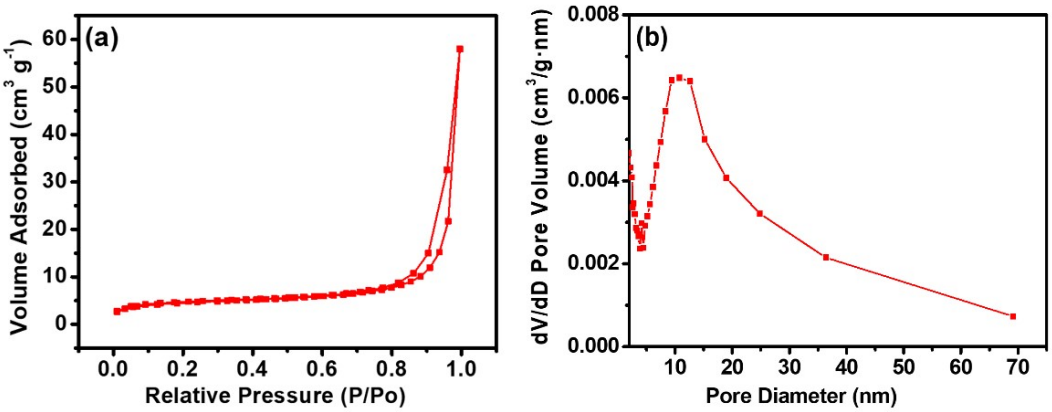

Fig. S8. N_2 adsorption-desorption isotherm of $(Co_1Ni_2)S_4$ and its pore size distribution

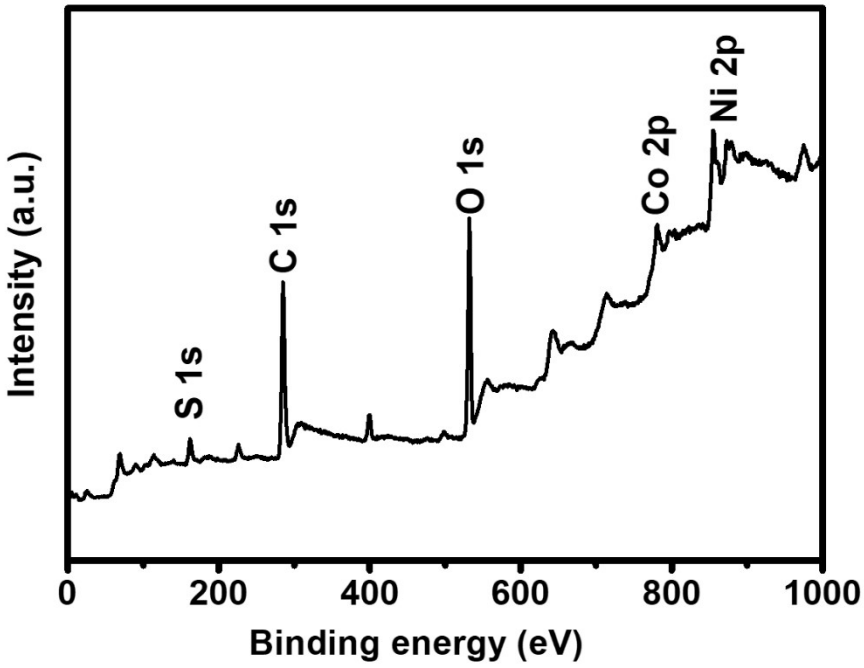

Fig. S9. XPS survey spectra for $(Co_1Ni_2)S_4$

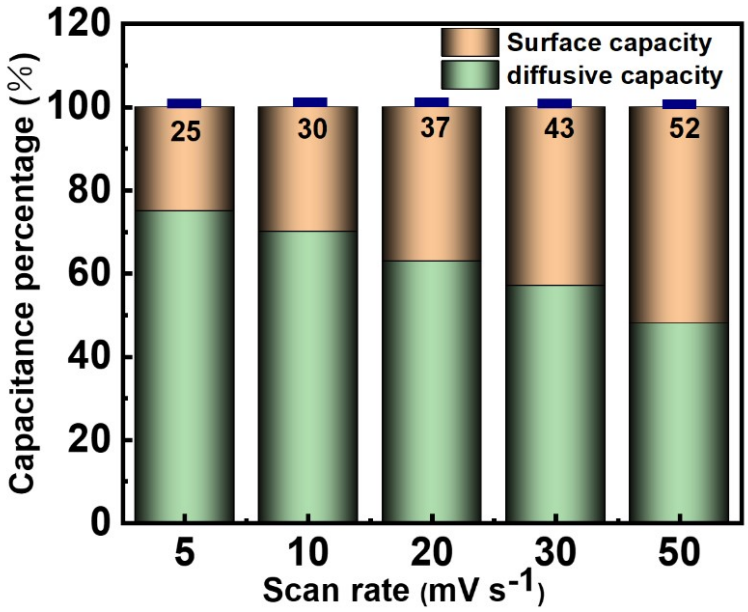

Fig. S10. The portions of capacitive contribution at various scan rates from 5 to 50 mV s^{-1} for $(Co_1Ni_2)S_4$

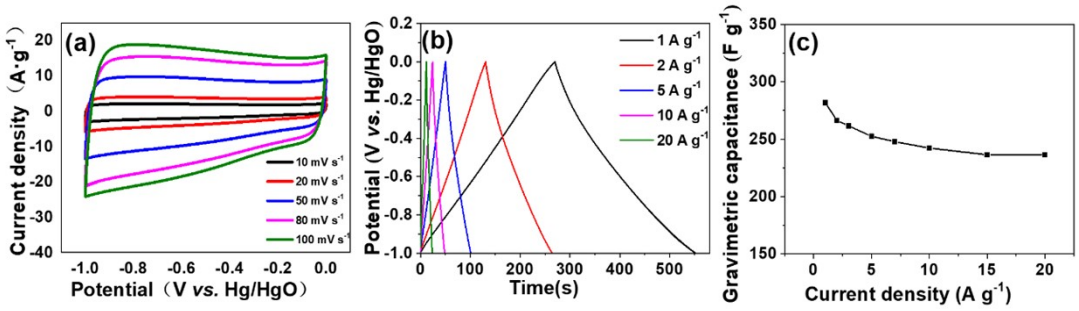

Fig. S11. Electrochemical capacitive performance of AC tested in three-cell configuration in 6.0 M KOH: (a) Cyclic voltammograms of AC at various scan rates, (b) Charge/discharge curve of AC at various current densities, and (c) Specific capacitance of AC at different current densities.

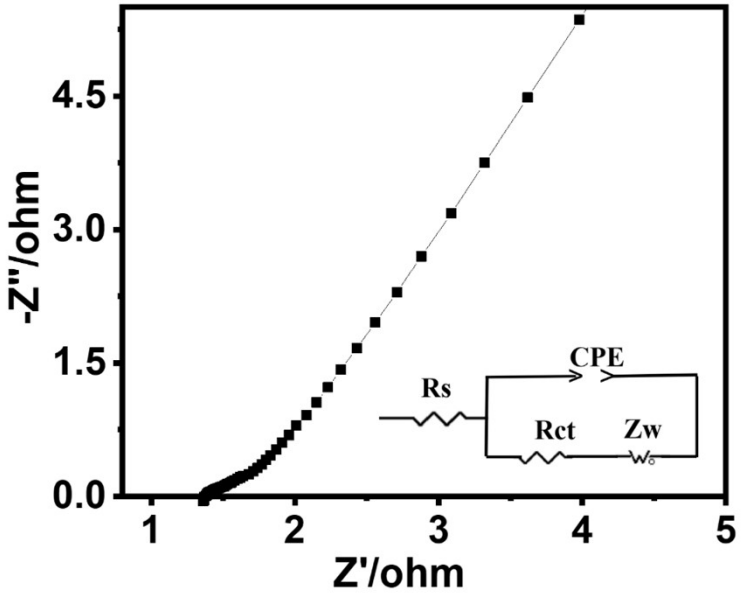

Fig. S12. Nyquist plot of the $(Co_1Ni_2)S_4$//AC device

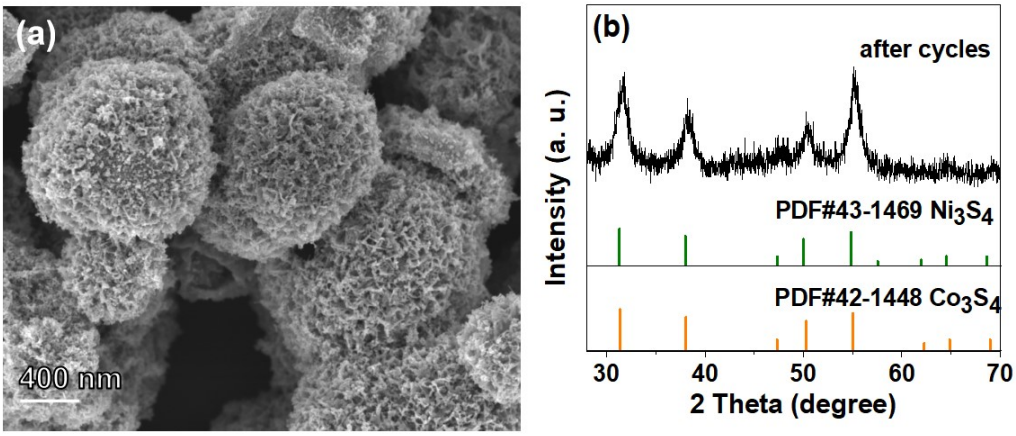

Fig. S13. (a) SEM image and (b) XRD patterns of $(Co_1Ni_2)S_4$ after 30,000 cycles.

Table S1. The atomic ratio of the $Co_xNi_{3-x}S_4$ powder determined by ICP-OES.

Sample	Co content W (%)	Ni content W (%)	Atomic ratio (Co:Ni)
$(Co_{1.5}Ni_{1.5})S_4$	24.86	22.79	0.42:0.39
$(Co_1Ni_2)S_4$	12.17	26.42	0.21:0.45
$(Co_{0.6}Ni_{2.4})S_4$	9.10	32.48	0.15:0.55

Table S2. Intertial resistance (R_s) and charge electrode resistance (R_{ct}) of different electrode materials.

Sample	R_{ct} (Ω)	R_s (Ω)
CoS	0.65	0.74
NiS	0.36	0.70
$(Co_{1.5}Ni_{1.5})S_4$	0.30	0.62
$(Co_1Ni_2)S_4$	0.27	0.61
$(Co_{0.6}Ni_{2.4})S_4$	0.36	0.68